Pembina Cardium CO$_2$ monitoring project: timelapse seismic analysis

Abdullah A. Alshuhail, Don C. Lawton, and Louis Chabot

ABSTRACT

Time-lapse analysis of the surface seismic dataset at the Violet Grove CO$_2$-EOR pilot project site shows no significant anomaly that can be attributed to the injected supercritical CO$_2$ between Phase I (March 2005) and Phase III (March 2007) of the project. However, the fixed-array vertical seismic profile (VSP) dataset exhibits small amplitude variations that may be associated with the CO$_2$ plume. The time-lapse analysis referred to here is based on the observation of amplitude and traveltime variations after the injection of approximately 40,000 t of CO$_2$ into the 1650 m deep, 20 m thick Cardium Formation over a period of two years. The ongoing analysis suggests that it would be hard to detect the CO$_2$ plume due to its being contained in very thin layers of relatively permeable sandstone members of the Cardium Formation. The seismic data, however, suggests that no leakage of CO$_2$ is taking place into shallower formations.

INTRODUCTION

The Violet Grove CO$_2$ enhanced oil recovery (EOR) program was established as a pilot project for CO$_2$-EOR in Alberta. At the site, supercritical CO$_2$ has been injected into the 1650 m deep, 20 m thick Upper-Cretaceous Cardium Formation since March 2005. As part of the pilot project, a time-lapse seismic program was designed and incorporated into the overall mitigation monitoring and verification (MMV) program. The seismic component of the MMV program is based on the acquisition, processing and interpretation of 2D and 3D surface seismic and 2D vertical seismic profile (VSP) datasets in an attempt to: (1) track the CO$_2$ within and around the reservoir, and (2) evaluate the integrity of the storage (Lawton et al., 2005; Chen et al., 2006; Coueslan et al., 2006). Time-lapse seismology is one of the most invaluable tools employed in reservoir characterization and monitoring in carbon capture and storage (CCS) projects around the world (Chapman et al., 2000; Arts et al., 2002; Brown et al., 2002; Terrell et al., 2002; Li, 2003; Miller et al., 2004). This report outlines some of the results from the latest (amplitude and traveltime) analyses of the time-lapse borehole and surface seismic datasets acquired during Phase I (March 2005) and Phase III (March 2007) of the project.

STUDY AREA

The Violet Grove CO$_2$-EOR pilot project site is located near the center of the Pembina Oil Field in the central plains of Alberta, about 120 kilometers southwest of Edmonton (Figure 1). The target of the CO$_2$-EOR program is the upper-sand unit of the Pembina River Member of the Cardium Formation (Figure 2). The Cardium Formation was deposited during a relative change in sea level approximately 88.5 MA, and is made up of sandstone sheets and a thin conglomerate layer sandwiched between thick black marine shales of the Blackstone Formation (below) and the Wapiabi Formation (above). It is thickest-deepest in the foothills and thins (and becomes shallower) as it transgresses into the northeast (Dashtgard et al., 2006). The Cardium Formation consists of two members:

Cardium Zone Member and Pembina River Member (Figure 2). The Pembina River Member is subdivided into three sand subunits (upper, middle and lower), and three shale subunits (upper, middle and lower). Maximum thickness of the Cardium Formation at the study area is 24 m, and the reservoir pressure and temperature are 19 MPa and 50°C, respectively.
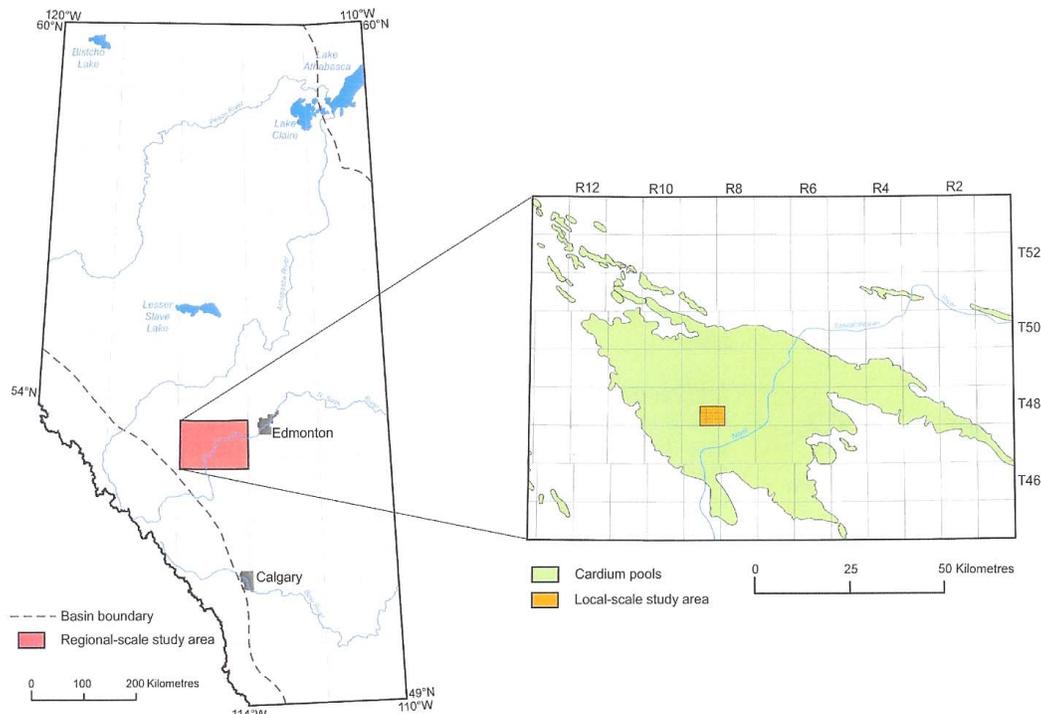
FIG. 1. Location map of the Pembina oil field. The study area is shown in orange rectangle (Dashtgard et al., 2006).

SEISMIC PROGRAM OVERVIEW

The seismic monitoring program at the Violet Grove CO_2-EOR site consisted of the acquisition, processing and interpretation of: (1) surface seismic dataset, and (2) vertical seismic profile (VSP) dataset. The surface seismic dataset is made up of two parallel, multicomponent 2D lines, 400 m apart and oriented east-west, and one orthogonal multicomponent 2D north-south line, intersecting near the CO_2 injector well (Figure 3). These three lines were each 3 km long with a receiver interval of 20 m, a source interval of 40 m, and a 2 kg dynamite source at a depth of 15 m. In addition, 8 triaxial geophones were cemented at 20 m intervals into an observation well at depths between 1497 and 1640m (Figure 3). The deepest geophone was located within the reservoir. All lines and borehole receivers were active throughout each survey (Phases I, II and III). Overall, the surface seismic program provided low-fold 3D subsurface coverage of the pilot site and the borehole seismic data provided high-resolution images of the target reservoir locally around the observation well. Table 1 gives a summary of the various data involved in each phase and the amount of CO_2 injected at the time of the data acquisition.
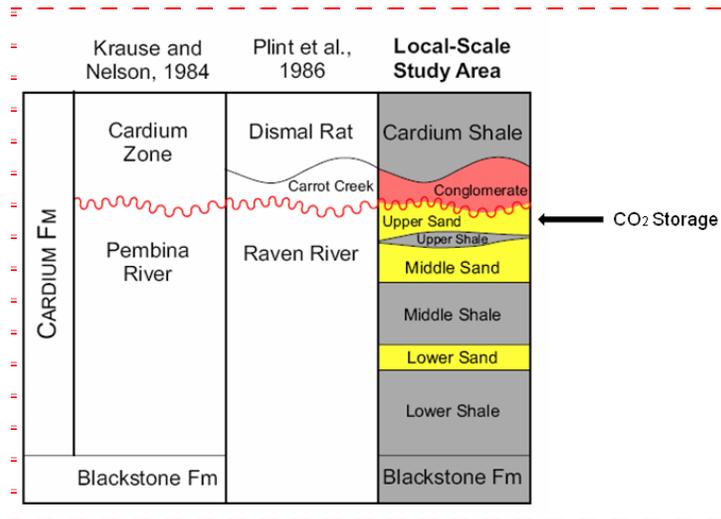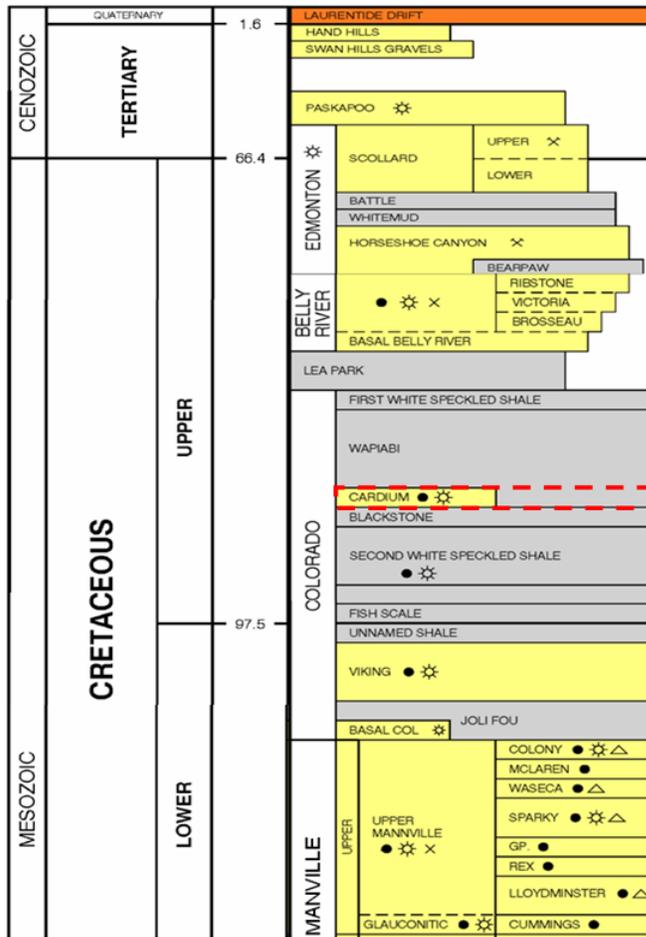
FIG. 2. Stratigraphic nomenclature of the Cardium Formation at the Pembina Field (Dashtgard et al., 2006), Cardium detail beneath.

During Phase III of the project, a new southwest-northeast trending 2D line (Line 6) and a vertical seismic profile (recorded in the western injector well) were added to the seismic program. However, by the time of the second monitoring survey, i.e. Phase III,

the program has already lost nearly 20% of the baseline shots due to additional infrastructure development that took place at the site.
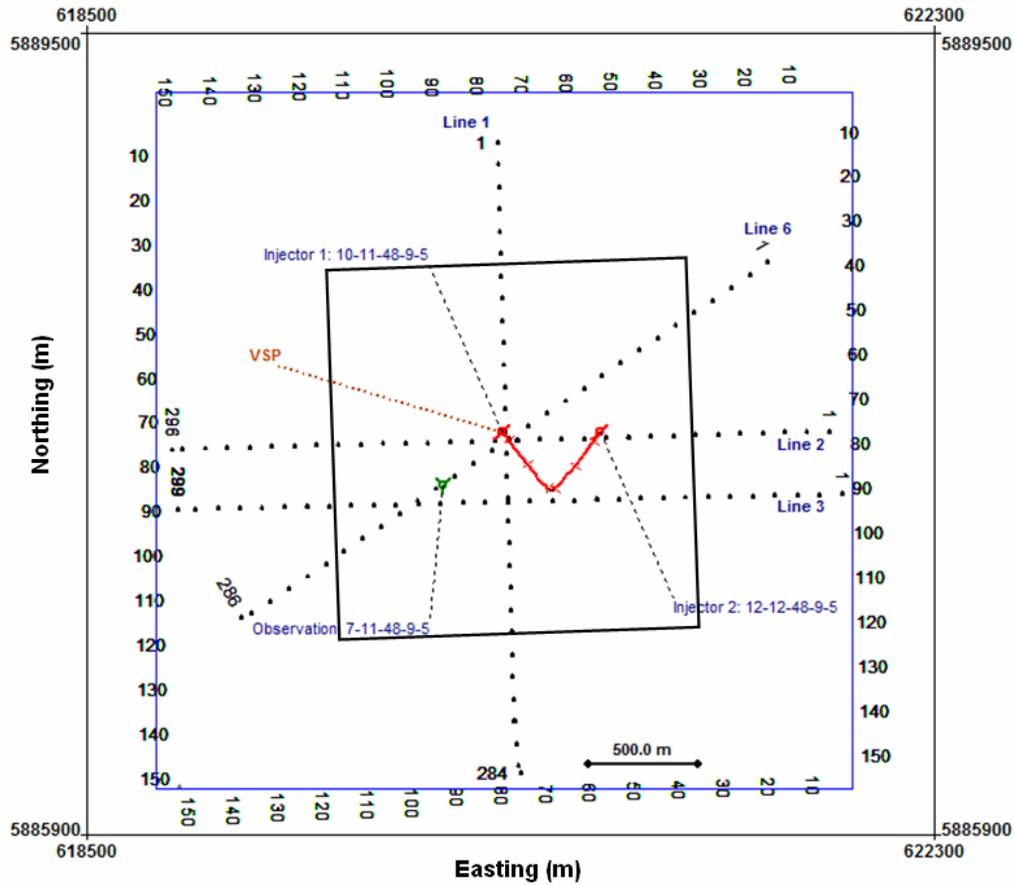
FIG. 3. Layout of surface seismic lines and location of the injector and observation wells. Rectangle shows 3D coverage.

Table 1. Summary of the seismic program at the Violet Grove CO_2-EOR.

	Seismic Data	Date	Amount of CO_2 Injected (tons)
Phase I (baseline)	(i) Line 1 (north-south). (ii) Lines 2 and 3 (east-west). (iii) Fixed-array VSP (8 geophones).	March 2005	0
Phase II (1st monitor)	(i) Line 1 (north-south). (ii) Lines 2 and 3 (east-west). (iii) Fixed-array VSP (8 geophones).	December 2005	~ 15,000
Phase III (2nd monitor)	(i) Line 1 (north-south). (ii) Lines 2 and 3 (east-west). (iii) Fixed-array VSP (8 geophones). (vi) Addition of: (1) high resolution 16-level VSP, and (2) 3 km southwest-northeast 2D line (Line 6).	March 2007	~ 45,000

SURFACE SEISMIC DATA INTERPRETATION

The surface seismic datasets were processed using a standard flow through to post-stack time migration. Identical flows were used for the baseline and monitor surveys after all non-repeated shots were first stripped from the datasets. The 2D lines shown in Figure 3 were initially processed independently and this was followed by a sparse 3D processing flow since all lines were live for all shots (shown by the rectangular outline in Figure 3). Data quality of the 2D PP data is good and high-amplitude reflections are obtained from a shallow coal horizon (Ardley Formation) and a deeper sandstone horizon (Viking Formation). The Cardium Formation is a low-impedance reservoir and the seismic response of the event is low amplitude, even on the monitor survey (Figure 4 (b)). The difference section (Figure 4 (c)) after the application of a matching filter above the reservoir shows no identifiable events at the Cardium or Viking event and the Ardley coal event has a small amplitude residual; the section is dominated by residual migration noise. Figure 5 shows the baseline (Phase I), second monitoring (Phase III) and the difference between the two for Line 2 (PP data) while Figure 6 shows those of Line 3. As in the case of Line 1, no distinct patterns are observed that can be attributed to the CO_2 plume. Nonetheless, the difference map from Line 3 (c) shows an interesting amplitude anomaly at the bottom of the injection well but this anomaly cannot be interpreted with high confidence at this time as similar features are observed within the difference section.

The converted-wave (PS) data for Line 1 are shown in Figure 7. Obviously, the quality of the PS data is lower than for the PP data and applying a matching filter above the reservoir was not successful in eliminating the difference due to the time-lapse acquisition footprints as can be seen, for instance, in the large residual amplitudes at the Ardley event. Overall, the difference section (Figure 7 (c)) does not exhibit any coherent pattern and therefore cannot reliably be interpreted to identify the CO_2 plume. The results from the other 2D PS data, i.e. Lines 2 and 3, are not presented in this report but they are similar in quality and findings to Line 1.

A broader image of the reservoir and the CO_2 plume may be constructed by looking at the horizons maps. Figure 8 (a) and (b) show a 3D visualization of the Ardley, Cardium and Viking horizons extracted from the 3D PP and PS datasets, respectively. Another possible way to identify the CO_2 plume is to look at the isochron difference between Phases I and III using two horizons: one above and another below the reservoir. This is because the injection of supercritical CO_2 would reduce the reservoir's incompressibility and slightly reduces its density, thus increasing the P-wave velocity. So, one would expect a small increase in the PP Ardley-Viking isochron between Phases I and III in the vicinity of the injection well. On the other hand, since the shear modulus is insensitive to fluid changes within the reservoir, the Ardley-Viking isochron between Phase I and III might exhibit a minor decrease in the case of the converted-wave (PS) due to the small increase in S-wave velocity. The isochron differences between Phases I and III in the case of the PP and PS datasets are displayed in Figure 8 (a) and (b). No consistent pattern can be observed by looking at the PP isochron difference (Figure 8 (a)) whereas the PS isochron difference (Figure 8 (b)) shows a more consistent pattern, i.e. a decrease in the Ardley-Viking isochron in the order of 2.5 ms in the northeast direction. This could be an indication that the CO_2 plume is migrating up-dip.
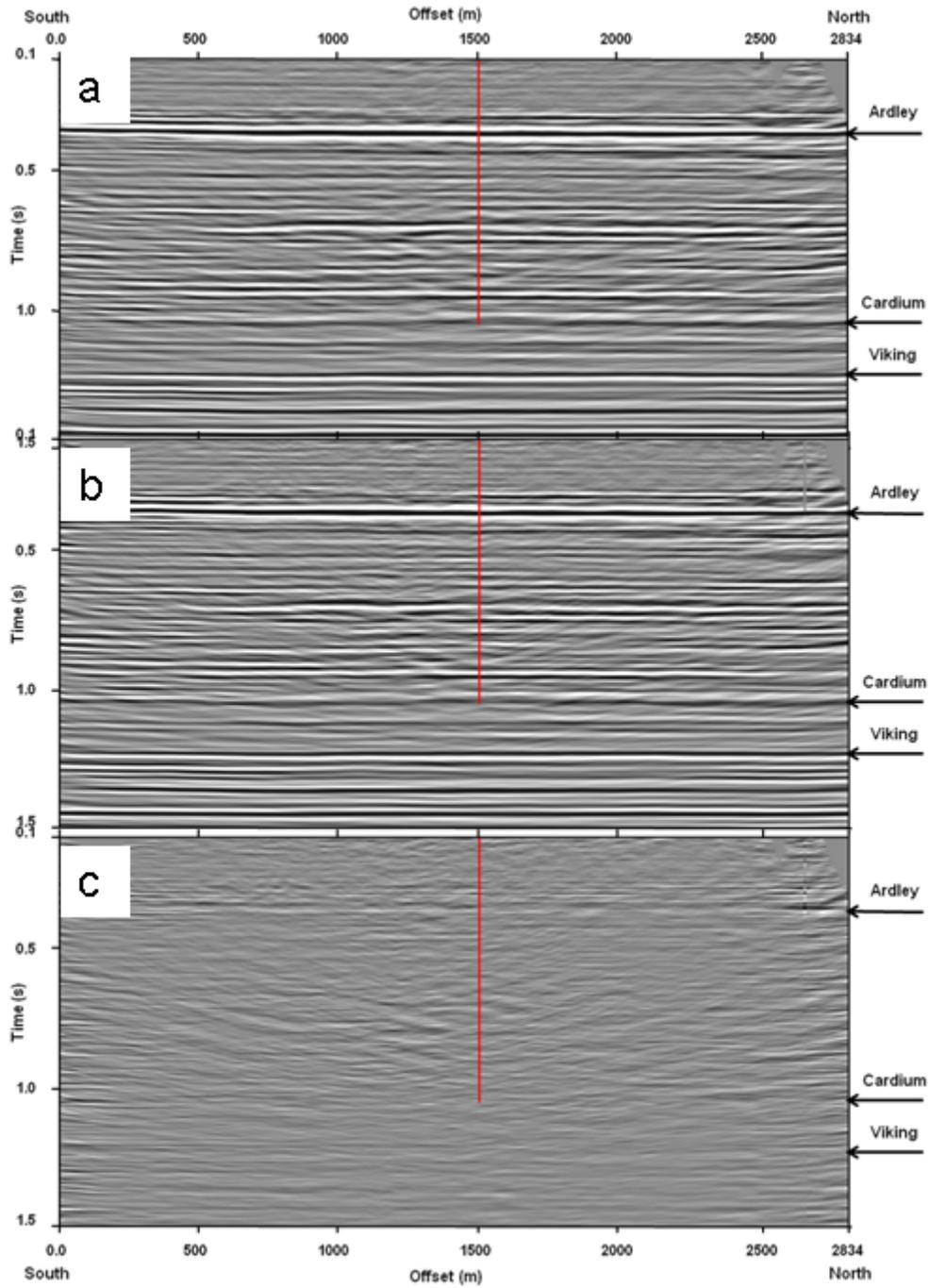
FIG. 4. Processed PP data from Line 1: (a) baseline (Phase I) data; (b) monitor (Phase III) data; (c) difference after application of matching filter above reservoir. Red line shows projection of CO_2 injector well.
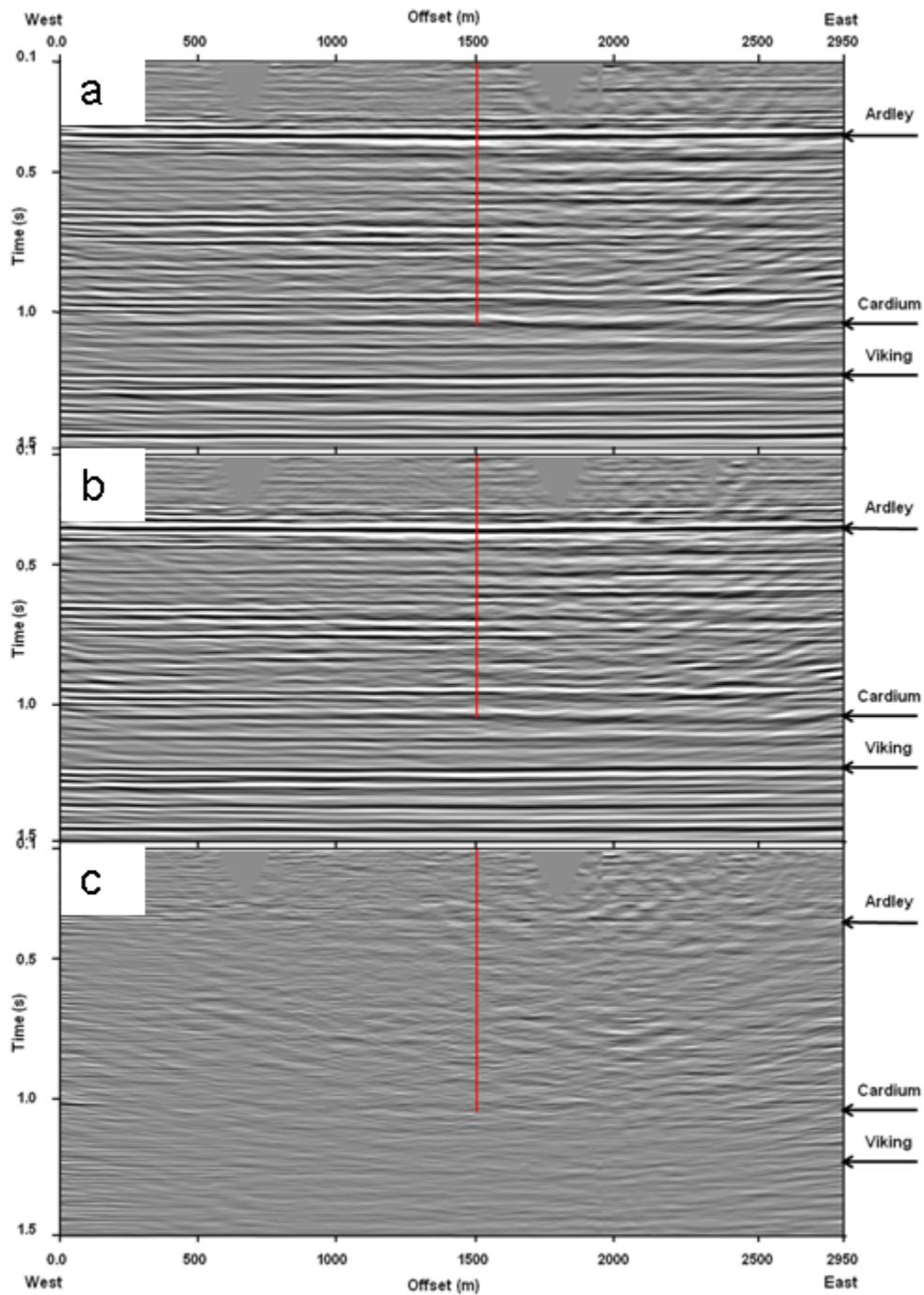
FIG. 5. Processed PP data from Line 2: (a) baseline (Phase I) data; (b) monitor (Phase III) data; (c) difference after application of matching filter above reservoir. Red line shows projection of CO$_2$ injector well.
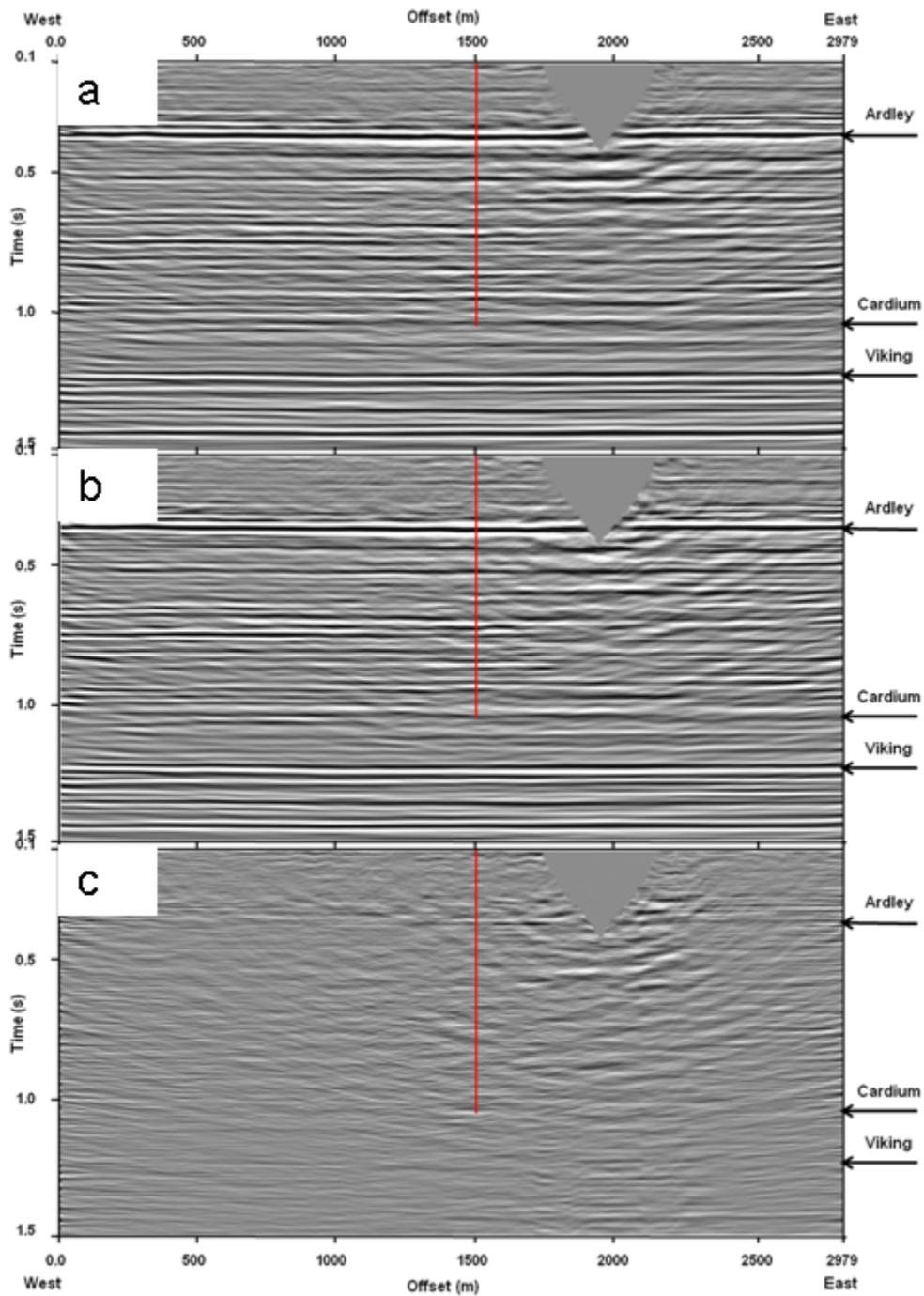
FIG. 6. Processed PP data from Line 3: (a) baseline (Phase I) data; (b) monitor (Phase III) data; (c) difference after application of matching filter above reservoir. Red line shows projection of CO_2 injector well. Note the small amplitude anomaly at the bottom of the injection well.
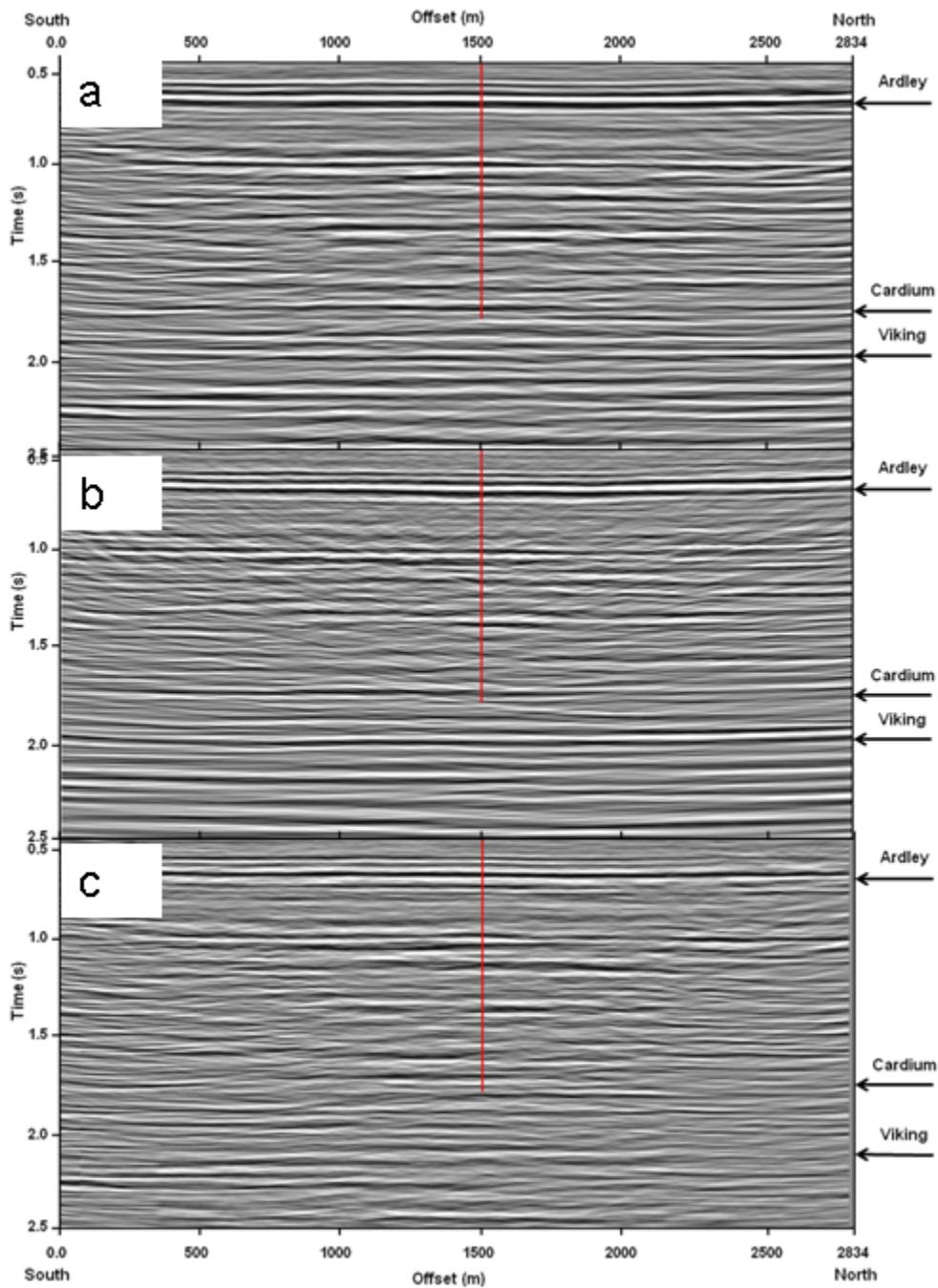
FIG. 7. Processed PS (converted-wave) data from Line 1: (a) baseline (Phase I) data; (b) monitor (Phase III) data; (c) difference after application of matching filter above reservoir. Red line shows projection of CO$_2$ injector well
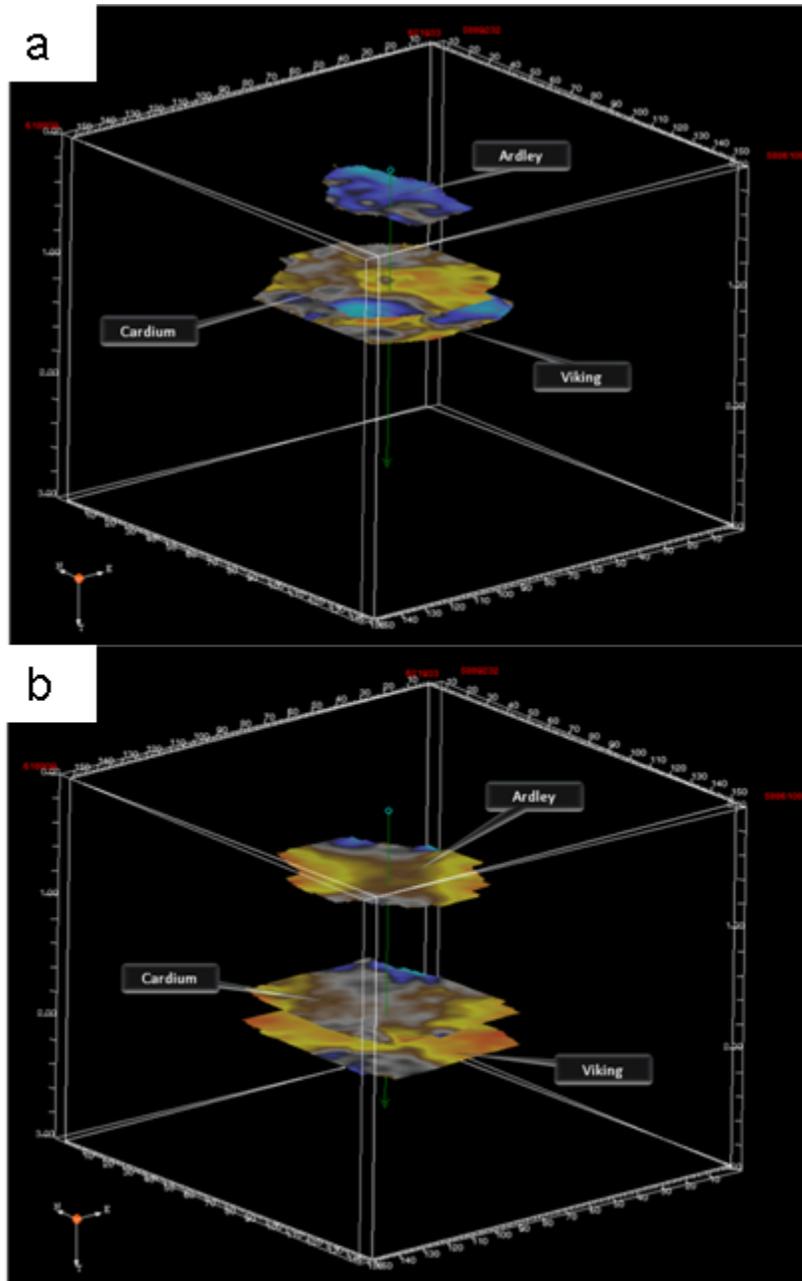
FIG. 8. A 3D visualization of the Ardley, Cardium and Viking horizons from: (a) the PP volume, and (b) the PS volume. The green line shows the trajectory of the observation well.
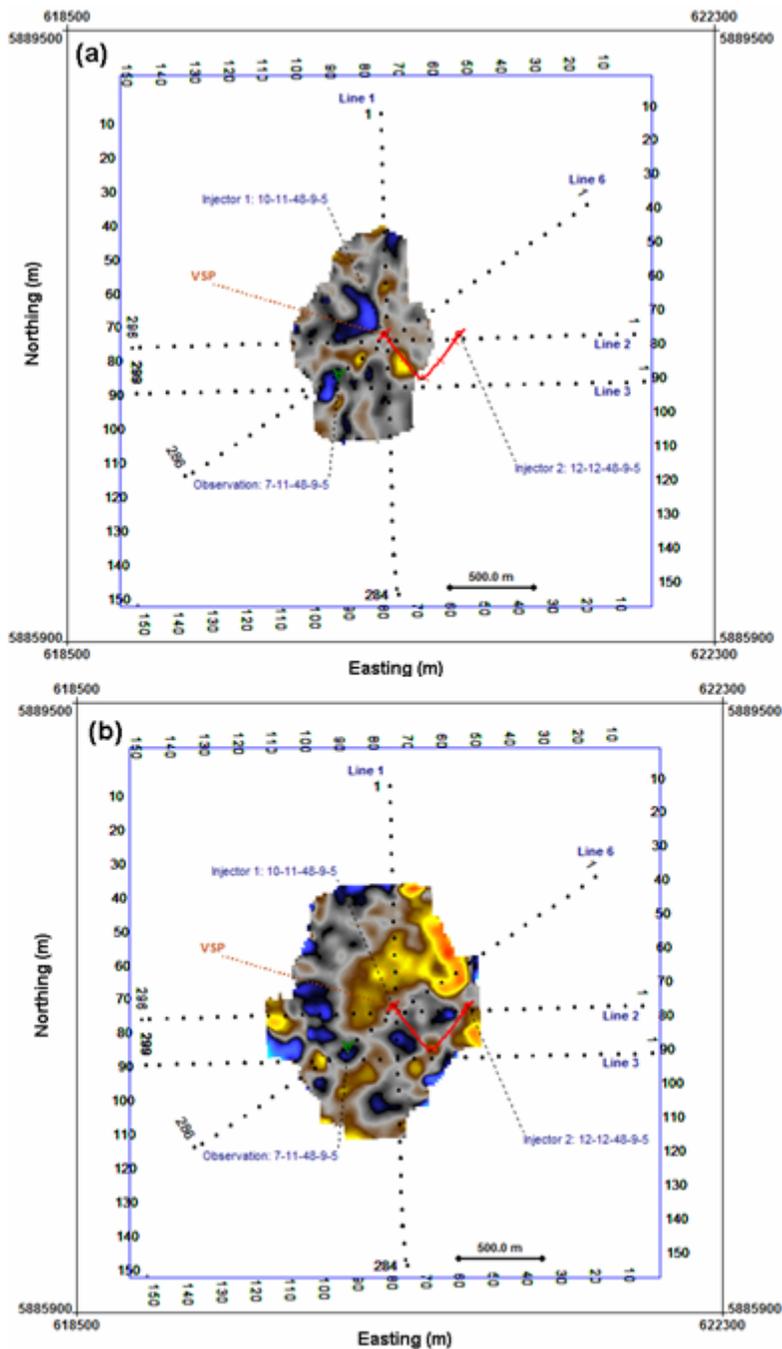
FIG. 9. Isochron difference between Ardley and Viking events for the Phase III and Phase I surveys: (a) PP data; (b) PS data. Blue colour indicates that there is an increase in the isochron difference (maximum 0.8 ms) in the case of PP and (maximum 1.1 ms) PS data. Red colour shows a decrease in the isochron difference (maximum -1 ms) for the PP and (maximum -2.5 ms) for the PS data. The PS isochron exhibits a more consistent pattern, i.e. a northeast decrease in the Ardley-Viking isochron.

VSP DATA INTERPRETATION

Since all shots of the surface seismic program were recorded into the downhole fixed-geophone array, each of the 2D lines was processed as a separate walkaway VSP following a flow developed for Phase II analysis (Coueslan, 2007). However, only 5 of the 8 receiver depths had full fidelity data on all three axes, so time-lapse VSP data was processed using only the vertical component, enabling 7 geophones to be utilized. The main pre-processing steps included application of shot statics, 60 Hz notch filter, and an 8-100 Hz bandpass filter. Wavefield separation of upgoing and downgoing arrivals was achieved using a median filter, followed by wave-shaping deconvolution design of the direct down-going wave. The separated upgoing P- and S-wavefields from each survey were migrated with the anisotropic velocity model and a 1D VTI Kirchhoff migration algorithm. The velocity model was the same as that developed during Phase II processing (Coueslan, 2007).

The time-lapse processed PP sections for Lines 1, 2 and 3 from the individual phases (I and III) are displayed in Figure 10 while the difference plots after cross-equalization, to minimize differences in the data unrelated to injection, are plotted in Figure 11. As expected, the VSP has higher bandwidth as reflections from the Cardium event are more visible in the VSP sections than in the surface seismic sections. Unfortunately, the lateral image of the Cardium Formation in the VSP data is limited to approximately 100 m due to the depth and limited vertical aperture of the geophone array in the observation well. Nonetheless, amplitude anomalies and traveltime differences north of Line 1 and east of Lines 2 and 3 can be observed in Figure 11. The amplitude and time structure plots from Line 1 show increases in Cardium event amplitude (Figure 12) and Viking event traveltime (Figure 13) at and north of the observation well between Phases I and III. The ongoing analysis suggests that these changes are caused by the migration of the CO_2 plume. Furthermore, the magnitudes of the amplitude variation and the traveltime delay at the Cardium and Viking events are within the range predicted by modelling (next section). Unfortunately, this observation cannot be supported by looking at Lines 2 and 3 as no consistent pattern can be identified in the amplitudes and time structures plots of these lines. Nonetheless, the observation that part of the CO_2 plume is migrating toward the observation well can be supported by fluid sampling, which shows that a certain amount of the injected CO_2 is sampled among the reservoir's fluids at the observation well.

ROCK PHYSICS AND MODELLING

CO_2 injection causes changes in fluid saturation and pressure in the reservoir. Modelling was undertaken for the Cardium Formation sandstones, assuming a relatively low porosity (~10%) and a cemented matrix. Increasing fluid compressibility by injecting CO_2 decreases the P-wave velocity in the reservoir by about 4% and density by ~1%, based on modified Gassmann's modelling and substituting a brine-light oil mix with supercritical CO_2 with up to 80% saturation. Zero-offset synthetic seismograms were generated to investigate changes in the P-wave seismic response for different CO_2 saturation and plume thicknesses (Figure 14). The results show subtle reflectivity changes at the Cardium Formation and a traveltime delay at the later high-amplitude Viking event. Figure 15 provides an insight into the predicted change in normalized RMS amplitude at the Cardium event as function of CO_2 saturation and reservoir thickness. The associated

time delay at the Viking event is illustrated in Figure 16. The predicted values in Figures 14 and 15 are within the range observed in the real data (Line 1) for the Cardium event amplitude (Figure 12) and Viking event time structure (Figure 13).
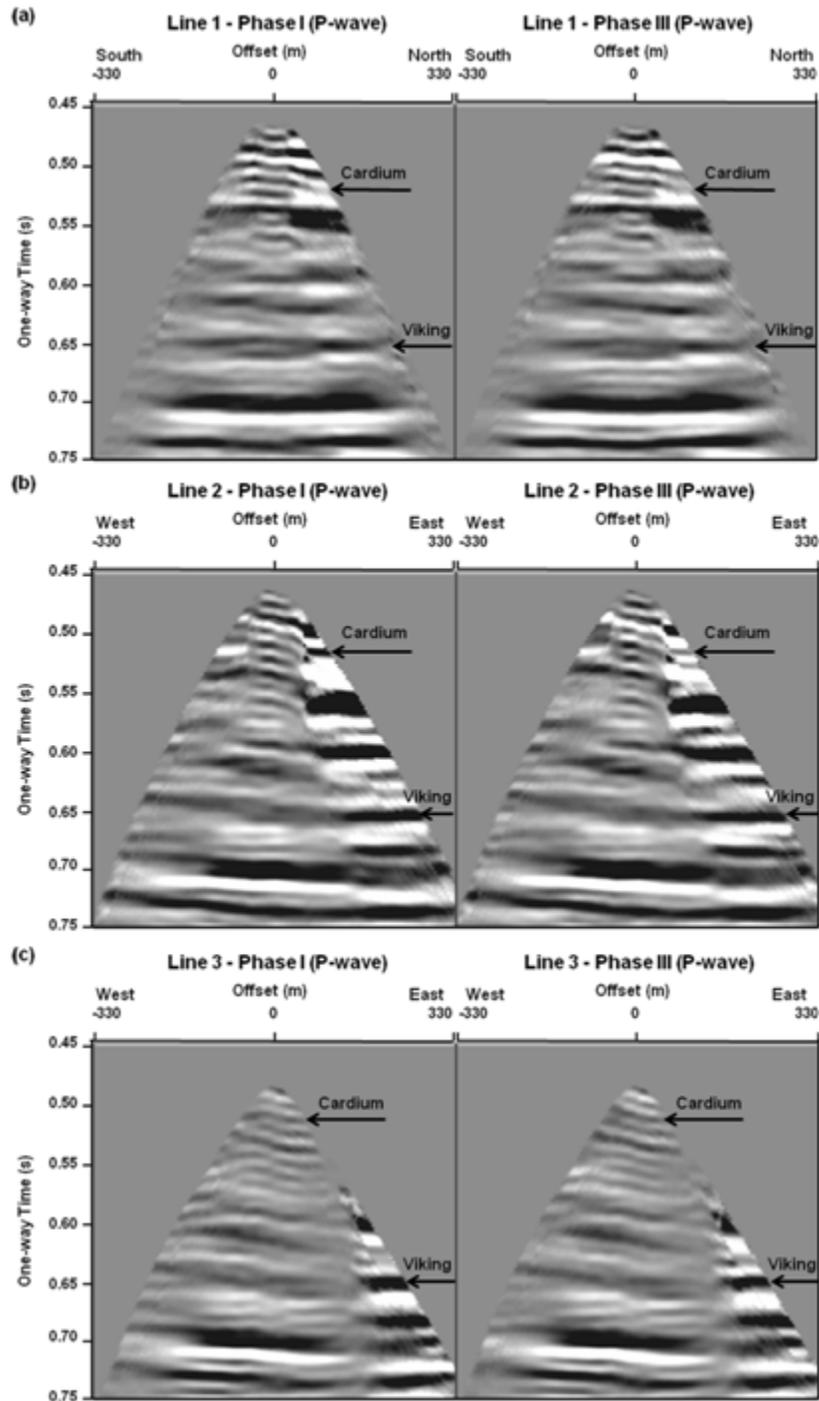
FIG. 10. Walkway PP VSP data from the observation well. (a) Line 1, Phase I and Phase III; (b) Line 2, Phase I and Phase III; and (c) Line 3, Phase I and Phase III.
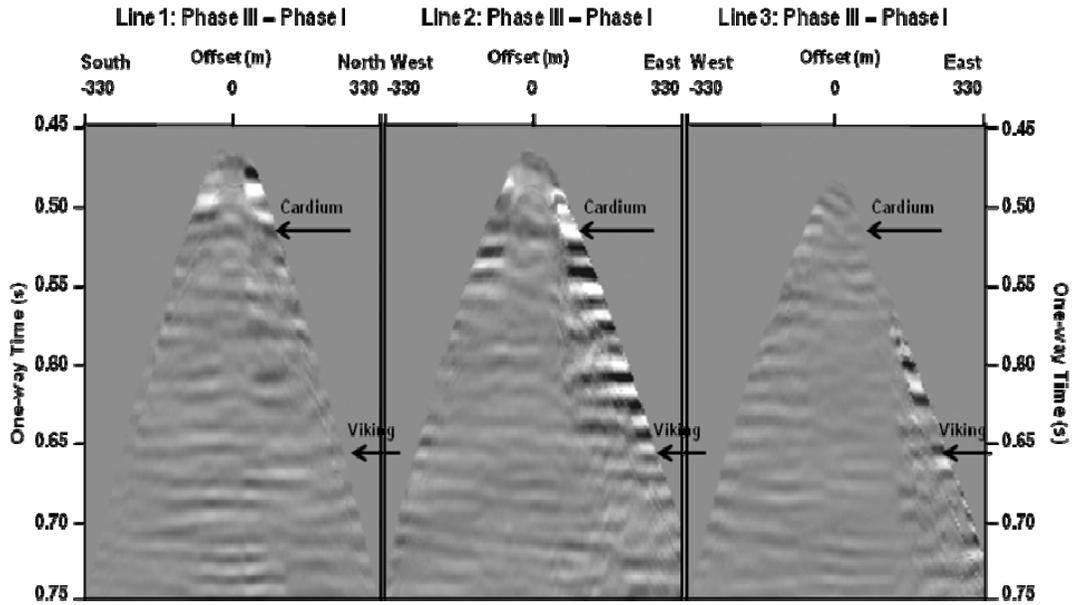
FIG. 11. Phase III – Phase I differenced walkway VSP data from the observation well. Line 1 (left), Line 2 (centre), and Line 3 (right).
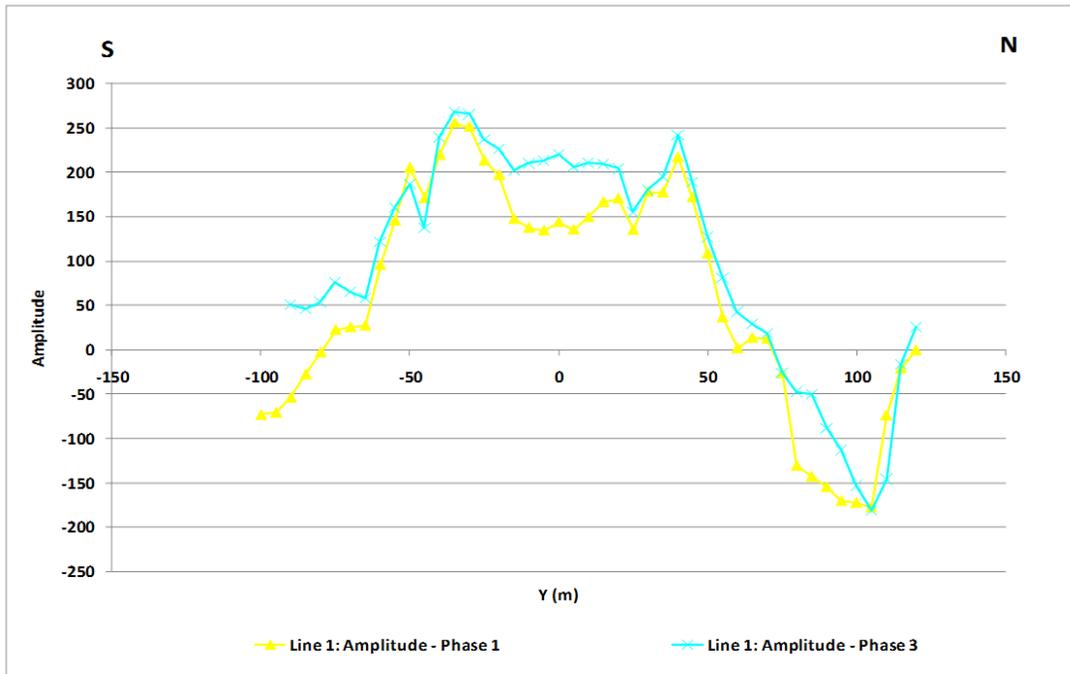
FIG. 12. Variations in Cardium event amplitude between Phase 1 and Phase III for Line 1. The observation well is located at Y = 0.
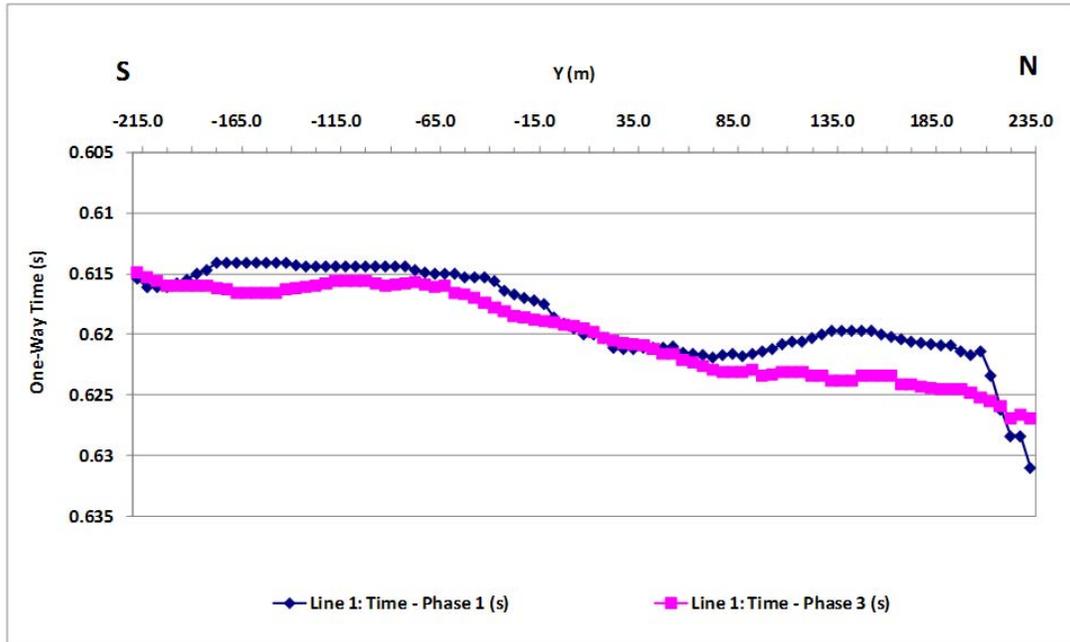
FIG. 13. Variations in Viking event (one-way) traveltime between Phase 1 and Phase III for Line 1. The observation well is located at Y = 0.
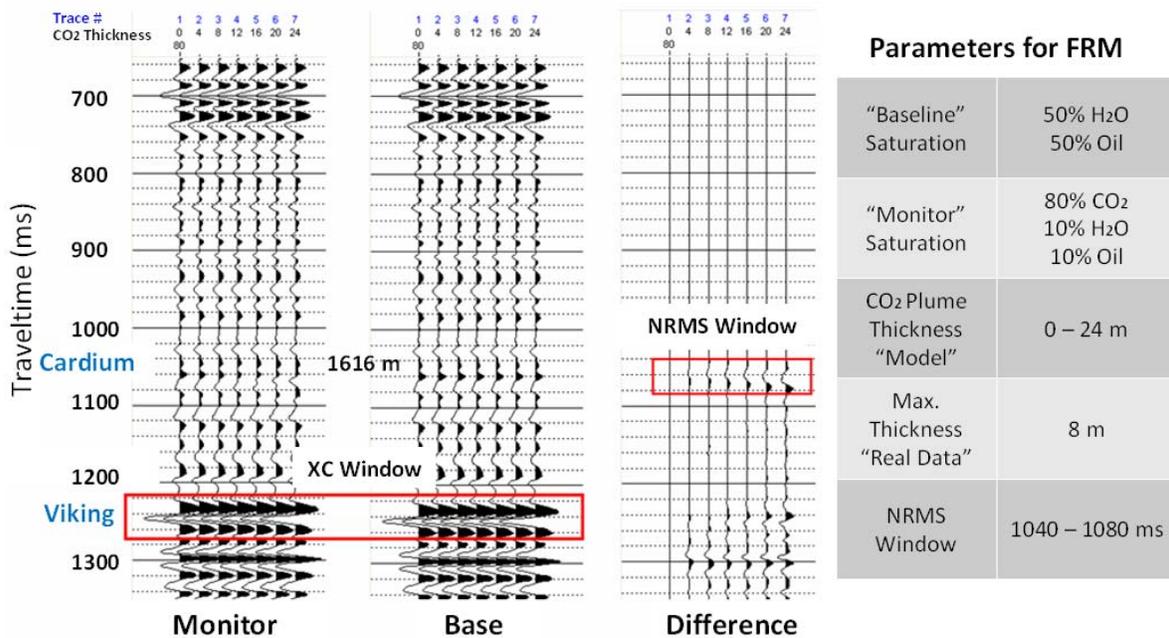
FIG. 14. Zero-offset seismic modelling of the effects of CO_2 saturation in the Cardium Formation. Traces from left to right in each panel show the results of increasing the CO_2 plume thickness from 0 to 24 m (full thickness of reservoir), and a constant 80% CO_2 saturation. The table to the right summarizes some of the fluid replacement modeling (FRM) parameters. The NRMS window and the XC windows where used to generate the matrices in Figures 15 and 16, respectively.
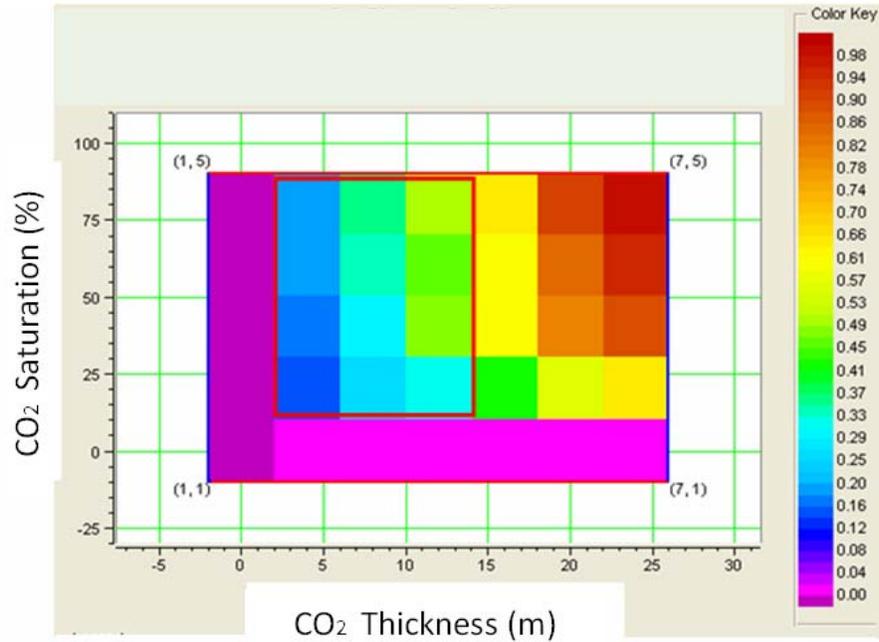
FIG. 15. Matrix of noise-free zero-offset synthetic analysis of normalized RMS amplitude difference (colour scale) at the Cardium formation. CO_2 varied from 0% to 80% and swept thickness varied from 0 m to 24 m. The red rectangle outlines the most likely reservoir conditions. CO_2 thickness is expected to be less than 10 m, which corresponds to NRMS difference < 0.55.
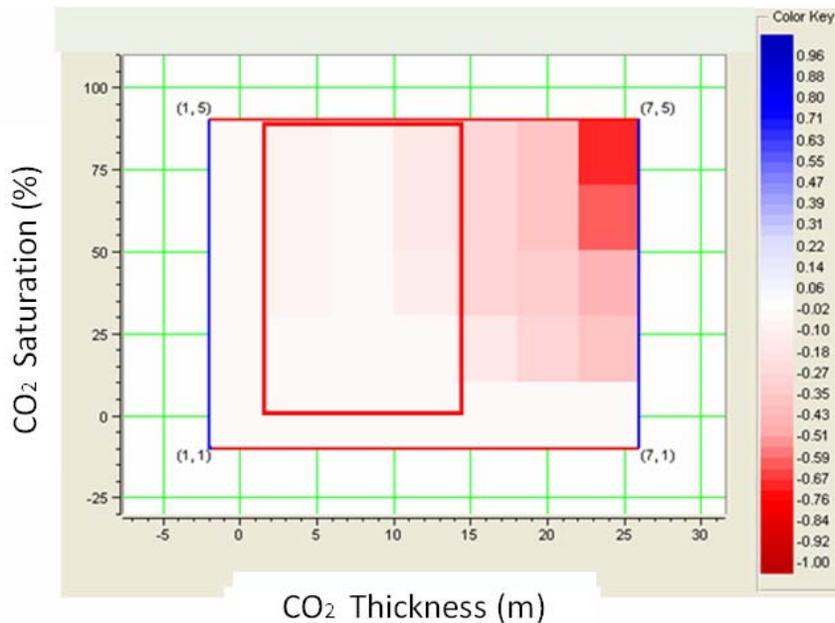
FIG. 16. Matrix of noise-free zero-offset synthetic analysis of time delay (colour scale) at the Viking formation by cross-correlation. CO_2 varied from 0% to 80% and swept thickness varied from 0 m to 24 m. The red rectangle outlines the most likely reservoir conditions. CO_2 thickness is expected to be less than 10 m, which corresponds to time delay < 0.25 ms.

DISCUSSION

The results presented in this report suggest that the time-lapse surface seismic program at the Violet Grove CO_2-EOR has not been successful in detecting the CO_2 plume after the injection of ~ 40,000 ton between Phases I and III. To a certain extent, the converted-wave (PS) component of the surface seismic program seems to provide a better image than the P-wave (PP) component as it revealed a subtle traveltime changes that might be attributed to the CO_2 presence in the reservoir. The most coherent results, though they lack spatial coverage, are those obtained by the fixed-array VSP dataset due to its higher frequency bandwidth and S/N ratio. The amplitude and traveltime changes as observed in Line 1 of the VSP dataset are small but they are consistent with those predicted from the rock physics modelling.

In summary, the lack of a significant and coherent anomaly at the reservoir zone in the time-lapse datasets, especially in the surface seismic dataset, may be due to one or more of the following factors:

1. The confinement of the CO_2 plume to thin sandstones with relatively high permeability within the Cardium.

2. The high noise level at the site, not all of which could be attenuated during the data processing flow, therefore resulting in a small residual noise level that might have obscured the weak anomaly.

3. The similarity in physical properties between the reservoir's fluids and the injected CO_2, which when added to the previous factor makes it even more difficult to identify the plume.

At the same time, the lack of a 4D changes above the reservoir indicates that the injected CO_2 is not leaking into shallower formations as seismic response would be more sensitive to the plume as it migrates upward toward the surface. Future work will involve looking into more robust measures, such as spectral decomposition.

ACKNOWLEDGEMENTS

REFERENCES

Arts, R., Eiken, O., Chadwick, A., Zweigel, P., Meer, L., and Zinszner, B., 2002, Monitoring of CO2 injected at Sleipner using time lapse seismic data: Abstracts of the 6th international conference on greenhouse gas control technology (GHGT-6), Kyoto, Japan.

Brown, L.T., T.L. Davis, and M. Batzle, 2002, Integration of rock physics, reservoir simulation, and timelapse seismic data for reservoir characterization at Weyburn Field, Saskatchewan [Exp. Abs.]: Society of Exploration Geophysicists, p. 1708-1711.

Chapman, M., S. Zatsepin, and S. Crampin, 2000, Time-lapse seismic changes in a CO_2 injection process in a fractured reservoir [Exp. Abs.]: Society of Exploration Geophysicists, p. 1536-1539.

Chen F., and Lawton D.C., 2006, Interpretation of baseline multicomponent seismic data at the Violet Grove CO2 injection site, Alberta, CSEG, Expanded Abstracts, 412-414.

Coueslan, M.L., D.C. Lawton, and M.J. Jones, 2006, Time-lapse monitoring of CO_2 EOR and storage with walkaway VSPs, 76th Annual International Meeting, SEG, Expanded Abstracts , 3130-3134.

Coueslan, Marcia, 2007, Processing and Interpretation of Time-lapse Vertical Seismic Profile Data from the Penn West CO2 Monitoring Project: M.Sc. Thesis, University of Calgary.

Dashtgard, Shahin E., Maja B.E. Buschkuehle, Mike Berhane, and Brent Fairgrieve, 2006, Local-Scale Baseline Geological Report for the Pembina-Cardium CO2-Enhanced Oil Recovery Site: Alberta Geological Survey.

Lawton, D., Coueslan, M., Bland, H., Chalaturnyk, R., and Jones, M., 2006, Seismic survey design for monitoring CO2 storage: Integrated multicomponent surface and borehole seismic surveys, Penn West Pilot, Alberta, Canada, Proc. of the 8th Int. Conf. on Greenhouse Gas Control Technologies, June 19-22, Trondheim, Norway, 5 p.

Li, Guoping, 2003, 4D seismic monitoring of CO2 flood in a thin fractured carbonate reservoir: The Leading Edge, **22**, 690-695.

Miller, Richard D., A. Raef, A. Byrnes, J. Lambrecht, and W. Harrison, 2004, 4-D high-resolution seismic reflection monitoring of miscible CO_2 injected into a carbonate reservoir in the Hall-Gurney Field, Russell County, Kansas [Exp. Abs.]: Society of Exploration Geophysicists.

Terrell, M.J., T.L. Davis, L. Brown, and R. Fuck, 2002, Seismic monitoring of a CO_2 flood at Weyburn field, Saskatchewan, Canada: Demonstrating the robustness of time-lapse seismology [Exp. Abs.]: Society of Exploration Geophysicists, p. 1673-1675.